JAVMA

^{18}F-sodium fluoride positron emission tomography provides pertinent additional information to computed tomography for assessment and management of tarsal pain in horses

Pablo Espinosa-Mur, DVM, DVSc, DACVS, DECVSMR[1]*; Mathieu Spriet, DVM, DACVR, DECVDI, DACVR-EDI[2]; Gabriel Manso-Diaz, DVM, MSc, PhD, DECVDI[3]; Stefanie Arndt, DVM, DrMedVet, DACVS[4]; Marcos Perez-Nogues, DVM, MSc, DACVS[2]; Javier Lopez-San Roman, DVM, PhD, DECVS, DECVSMR[3]; Ricardo Garcia-Mata[3]; Scott A. Katzman, DVM, DACVS[2]; Larry D. Galuppo, DVM, DACVS[2]

[1]Department of Clinical Studies, Ontario Veterinary College, University of Guelph, Guelph, Ontario, Canada
[2]School of Veterinary Medicine, University of California-Davis, Davis, CA
[3]Facultad de Veterinaria, Universidad Complutense de Madrid, Madrid, Spain
[4]Department of Clinical Sciences, Cummings School of Veterinary Medicine, Tufts University

*Corresponding author: Dr. Espinosa-Mur (espinosp@uoguelph.ca)

Received April 15, 2023
Accepted July 11, 2023

doi.org/10.2460/javma.23.03.0164

OBJECTIVE
To assess the value of ^{18}F-sodium fluoride (^{18}F-NaF) positron emission tomography (PET) for imaging the tarsus and proximal metatarsus and compare it with CT and lameness evaluation.

ANIMALS
25 horses with lameness localized to the tarsal and proximal metatarsal regions that underwent ^{18}F-NaF PET/CT between 2016 and 2021.

METHODS
^{18}F-NaF PET and CT images were retrospectively independently evaluated by 3 observers. Standardized uptake values (SUV) were used to characterize ^{18}F-NaF uptake. Correlation between PET and CT findings with subjective and objective maximum (Max-D) and minimum pelvic height lameness data was estimated.

RESULTS
The inter-observer Kappa-weighted value (κ) was higher for PET (κ = 0.66) than CT (κ = 0.6). CT and PET scores were fairly correlated (R = 0.49; $P < 0.05$). PET SUVratio (SUV of the main lesion/SUV talus) had the highest correlation with Max-D (R = 0.71; $P < .05$). PET and CT scores for the plantar region were significantly higher in Quarter Horses ($P < .05$) and showed consistently higher correlation with objective lameness data (CT plantar grade - Max-D [R = 0.6; $P < .05$], PET plantar grade - Max-D [R = 0.47; $P = .04$]) than other regions of the distal tarsal joints. Three Warmbloods presented marked uptake at the medial cochlea of the distal tibia.

CLINICAL RELEVANCE
PET had a moderate correlation with CT for assessment of tarsal lesions. The degree of PET uptake can help differentiate active versus inactive lesions. Specific location of the uptake is important in determining clinical relevance.

The tarsus is commonly associated to unilateral or bilateral hind limb lameness in horses.[1] Several disorders can induce tarsal pain, these include osteoarthritis, osteochondritis dissecans, cystic lesions, fractures and enthesopathy among others.[2] For the proximal metatarsal region, the enthesis of the proximal suspensory ligament (PSL) into the plantar aspect of the third metatarsal bone and the suspensory ligament itself are very frequently identified as source of pain and thus lameness.[3] In some cases, a combination of pathologies such arthritis of the distal tarsal joints and desmitis of the PSL can be seen in the same horse.[3] However, multiple reports have demonstrated a significant overlap of all these pathologies when performing tarsal and subtarsal diagnostic analgesia.[4,5] The proximity of the anatomic structures and diffusion of anesthetic solutions are the most plausible explanation for this lack of specificity.[5] Imaging modalities that could help differentiate active processes from chronic and incidental lesions is of paramount importance in cases of tarsal and proximal metatarsal lameness.

Routinely used imaging tools for the tarsal and proximal metatarsal region include ultrasound and radiographs. Advanced imaging modalities include scintigraphy, CT and MRI. Increased radiopharmaceutical uptake (IRU) on scintigraphy has good correlation with distal tarsal pain in horses[6]; however, it offers poor anatomical details when compared to other techniques.[7] MRI has been shown better correlation and anatomic detail than ultrasound to detect pathological changes in the proximal suspensory region including the presence of adhesions between the PSL and adjacent structures.[8]

Positron emission tomography (PET) is a nuclear medicine imaging technique that has recently become available for use in the horse.[9–11] Compared with scintigraphy, PET has the advantage of providing cross sectional imaging, resulting in more specific localization of lesions.[9] ^{18}F-sodium fluoride (^{18}F-NaF) is an excellent marker of bone turnover due to the fluoride being taken up by the exposed hydroxyapatite crystals, similar to the ^{99m}Technetium-methylenediphosphonate (^{99m}Tc-MDP) radiotracer used in bone scintigraphy.[12–14]

The goals of this study were to describe the findings of ^{18}F-NaF PET in the tarsal and proximal metatarsal regions and to compare with CT findings in a clinical population of horses. Additionally, we studied the potential associations between the severity and distribution of the PET and CT findings with objective and subjective lameness scores. We hypothesized that there would be good agreement between PET and CT findings but that PET would show higher correlation than CT with lameness scores. A secondary hypothesis was that the distribution of ^{18}F-NaF uptake would differ between breeds.

Methods

Horses admitted for lameness to the Veterinary Medical Teaching Hospital of the University of California-Davis that underwent 18F-NaF PET/CT of the tarsal-metatarsal region were included. Signalment, primary activity, clinical history and lameness were recorded. The lameness grade was subjectively assessed using the reported grading scale by the American Association of Equine Practitioners (AAEP grade).[15] When available, presence and degree of lameness was objectively assessed by measuring maximum (Max-D) and minimum (Min-D) pelvic height differences between right and left halves of the stride using commercially available inertial sensors (Lameness Locator; Equinosis Q).

PET/CT image acquisition

PET and CT images were acquired under the same anesthetic period using a previously described protocol.[16] Briefly, horses were premedicated with xylazine (0.5 mg/kg, IV). Anesthesia induction was performed using ketamine (2 mg/kg, IV) and midazolam (0.05 mg/kg, IV) and anesthesia was maintained using isoflurane. For PET scan images acquisition a systemic dose of approximately 20 mCi (740 MBq) of ^{18}F-NaF was administered intravenously 60 minutes prior to imaging. Horses were imaged in lateral recumbency under general anesthesia with a compact PET scanner with a 22.5 cm bore, 22 cm axial field of view, and 2 mm spatial resolution (PiPET; Brain Biosciences). A urinary catheter was placed. Imaging started immediately after proper positioning of the horse on the table. The acquisition time for each scan was 10 to 15 minutes. CT imaging was performed immediately after the PET scan under the same anesthetic period. A 16-slice GE Lightspeed scanner (GE Healthcare) was used with field of view of approximately 20 to 30 cm, matrix size of 512 X 512, 0.6 mm slice thickness and image reconstruction with a bone algorithm.

Image analysis

The PET images were coregistered with the CT images using a dedicated software (Galatea; BrainBiosciences).[17] Fusion of the coregistered PET and CT images was performed using a DICOM viewer (Horos) for image analysis.

A customized table including 113 regions with all the joints and main ligamentous attachments from the distal tibia to the proximal metatarsal region was generated and used for image grading **(Supplementary Table S1)**. For each region, PET and CT images were independently graded by 3 observers (2 board-certified veterinary radiologists and a board-certified veterinary surgeon). The uptake in each region was graded as normal (0), mild (1) or moderate to severe (2) by each observer. For each area with increased uptake, attenuated corrected maximal standardized uptake value (SUVmax) were measured. SUV was defined as the tissue concentration of tracer divided by the decay-corrected injected activity and body weight. The Horos circular ROI tool was used and the ROI were drawn centered on the area of the highest uptake. A second similarly shaped and sized ROI was drawn on the talus where subjectively normal uptake was present. The SUVratio was then calculated by dividing the SUVmax of the lesion by the SUV of the talus. The CT abnormalities were further described by each observer as sclerosis, bone resorption, periarticular remodeling, fragmentation, cyst like lesion, joint fusion, or enthesophytosis. In cases with more than 1 CT lesion type the most severe was selected as representative for the region. The graded PET and CT images were then reviewed together by the 3 observers and consensus on final agreement was obtained in cases of major discrepancies (regions with 2 grades differences between observers). For the remaining regions, the median grade was calculated and used for the later statistical analysis.

The tarsus and proximal metatarsus were divided in 7 main regions including the tibiotarsal joint (TTJ), talocalcaneal joint (TCJ), proximal intertarsal joint (PITJ), distal intertarsal joint (DITJ), tarsometatarsal joint (TMTJ), metatarsal bones (MTB; second, third, and fourth metatarsal bones excluding their proximal articular portion and the enthesis of the suspensory ligament) and proximal suspensory attachment (PSL). Using the median grades of the detailed table (Supplementary Table S1) an overall CT

and PET score of normal (0), mild (1) or moderate to severe (2) was determined for each region. The SUVmax (highest SUVmax value) and SUVratio of the main lesion were also calculated.

Lesions of the distal intertarsal and tarsometatarsal joints were subdivided into 4 regions (dorsal, plantar, medial, and lateral) and regrouped under "distal tarsal joints" for statistical analysis.

Statistical analysis

Using the detailed table with the 113 separate regions (Supplementary Table S1), Weighted Kappa values (κ) were calculated among the 3 observers for PET and CT scores. Kappa coefficients were interpreted as follows: values ≤ 0 as indicating no agreement, values 0.01 to 0.2 as none to slight, 0.21 to 0.4 as fair, 0.41 to 0.6 as moderate, 0.61 to 0.8 as substantial, and 0.81 to 1 as almost perfect agreement.[18]

Additionally, the overall PET and CT correlation for the 113 regions was estimated using the Spearman rank correlation test (R). For the distal tarsal joints, the agreement between CT and PET for each region (dorsal, plantar, medial, and lateral) was calculated using the weighted Kappa value. Tests of symmetry were also performed.

For each CT lesion type (sclerosis, bone resorption, periarticular remodeling, fragmentation, cyst like lesion, joint fusion or enthesophytosis) the SUVmax values and SUVratio were compared using a Wilcoxon 2 sample test. The potential association between breed with PET and CT scores of the distal tarsal joints was estimated for each region (dorsal, plantar, medial, and lateral) using the Wilcoxon signed-rank test. The Spearman correlation test was used to estimate the potential correlation between age, AAEP grade, Max-D, and Min-D with the PET and CT scores for each region (dorsal, plantar, medial, and lateral). Additionally, the association between the 3 lameness related variables (AAEP grade, Max-D, and Min-D) with the variables SUVmax and SUVratio of the main lesion was analyzed using a Spearman's rank correlation test. The Spearman correlation test was interpreted as follows: values ≤ 0 as indicating no correlation, values 0.1 to 0.29 as poor, 0.3 to 0.59 as fair, 0.6 to 0.79 as moderate, 0.8 to 0.99 as very strong and 1 as perfect correlation.[19]

Statistical significance was set at $P < .05$.

Results

A total of 25 horses (13 geldings, 10 mares, 2 stallions) met the inclusion criteria. Median age was 11 years old (range, 5 to 17 years). Breeds included Quarter Horses (n = 12), Warmbloods (10), Thoroughbreds (2), and Andalusian (1). For statistical analysis, the Warmbloods, Thoroughbreds and Andalusian were regrouped under the term "Sport Horses." Twenty-three horses presented with lameness localized to the tarsal-proximal metatarsal region. Included horses had a negative distal limb block and a positive block of the tarsal or proximal metatarsal region performed by the referring veterinarian or the referral institution. One horse presenting with a large distal tibial cystic lesion was sound during lameness examination. Another horse that initially responded to the perineural analgesia of the deep branch of the lateral plantar nerve later responded to perineural anesthesia of the lower limb. This horse presented with bilateral fragmentation of the proximal tubercle of the talus and was scanned to rule out pathology associated with the proximal suspensory ligament.

Bilateral PET/CT imaging of the tarsal and proximal metatarsal region was performed in 21 horses, whereas unilateral imaging was acquired in 4 cases, resulting in a total of 46 limbs included in the study. Eight of the horses for which both tarsi were imaged were considered bilaterally lame, resulting in the inclusion of 31 lame limbs and 15 nonlame limbs.

Total anesthesia time from induction to the arrival in the recovery stall was 129 minutes (median; range, 100 to 140 minutes). No complications during anesthesia or recovery were recorded for any of the cases.

PET and CT comparison

When comparing the scores from the 3 observers for the 113 anatomical regions, the inter-observer agreement scores were substantial for PET (κ = 0.66 [0.45 to 0.69], median [range]) and moderate for CT (κ = 0.6 [0.32 to 0.63]). When comparing CT with PET scores for each of the 113 anatomical regions, the resulting Spearman rank correlation coefficient was 0.49 ($P < .05$). The top 20 anatomical regions with the most common abnormalities for both PET and CT are presented **(Supplementary Tables S2 and S3)**. The most common PET abnormality was part of the TMTJ with the plantar subchondral bone of proximal MT3. The rest of the top 20 PET abnormalities mainly involved the subchondral bone of the DITJ and TMTJ, but also included 2 sites of ligament attachments: the lateral proximal suspensory attachment (18th) and the tertial interosseous ligament attachment on the third metatarsal bone (17th). The most common CT abnormalities was irregularity at the lateral origin of the suspensory ligament, but this only ranked as 18th for PET abnormalities. The second most common CT abnormality also ranked as second most common on PET and was part of the DITJ (dorsal proximal subchondral bone of the third tarsal bone). The remainder of the top 20 CT abnormalities were all related to subchondral bone of the DITJ or TMTJ.

For the distal tarsal joints, the weighted Kappa value between PET and CT scores for the dorsal, lateral and medial regions was moderate (0.46), substantial (0.78), and fair (0.37), respectively. For the plantar region the weighted Kappa value was considered substantial (0.66). The test of symmetry for the plantar and medial regions revealed that the PET significatively showed higher scores when compared to CT ($P < .05$). For the dorsal ($P = .11$) and lateral ($P = .31$) regions the test of symmetry did not reveal asymmetric discrepancies between CT and PET.

Imaging findings

The main lesion detected on PET scan was located to the TTJ in 6 tarsi, to the TCJ in 1 tarsus, to the PITJ in 3 tarsi, to the DITJ in 8 tarsi, to the TMTJ

in 6 tarsi, to the MTB in 2 tarsi, and to the PSL in 4 tarsi. For the remaining 16 tarsi, a main lesion was not clearly identified. For the cases with the main lesion localized to the TTJ, 3/6 presented with marked uptake (mean SUVmax 41.1) at the medial cochlea of the tibia with subtle changes on CT **(Figure 1)**.

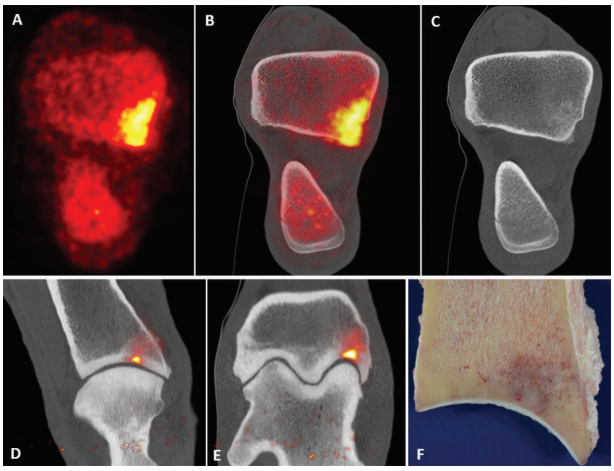

Figure 1—Positron emission tomography (PET; A), PET/CT (B) and CT (C) transverse images at the level of the distal tibia in a 13-year-old Warmblood gelding presenting after an acute onset of severe right hind limb lameness (4/5) 4 weeks before admission (3/5 lame on admission). Images show marked uptake at the distal and medial portion of the tibia affecting trabecular and cortical bone. On the CT images, there is mild trabecular sclerosis and periosteal reaction of the caudal tibial cortex (D). There is focal mild demineralization of the subchondral bone plate of the medial cochlear groove at the site of the highest PET uptake (D and E). After 9 months of conservative management and lack of improvement, the owners elected humane euthanasia. The post-mortem exam showed moderate osteonecrosis and fibrosis with cartilage degenerations at the articular surface of the medial trochlear groove (F).

Two out of 6 tarsi presented with fragmentation of the proximal tubercle of the talus and mild uptake (mean SUVmax = 23.2) and 1/6 had a large subchondral bone cyst at the distal portion of the tibia (SUVmax = 26). The tarsus with lesion localized to the TCJ had severe uptake (SUVmax = 46.6) at the medial facet. CT showed moderate bone resorption and peri-articular new bone. One of the 3 horses with the main lesion localized to the PITJ presented severe uptake (SUVmax 38.1) at the distal portion of the talus with CT showing a small cystic lesion at this site. The remaining 2 tarsi with the proximal intertarsal joint affected had mild degenerative changes on CT with mild uptake (mean SUVmax = 25.2). Seven out of 8 tarsi with the main lesion localized to the DITJ had uptake that ranged between mild and moderate (mean SUVmax = 24.4). On CT, a combination of degenerative changes including periarticular new bone, bone resorption, sclerosis and joint fusion were detected **(Figures 2 and 3)**. Subchondral bone abnormalities were more frequently reported than changes at the interosseous enthesis. The remaining case had a small

Figure 2—Sagittal (left) and transverse (right) CT (A and B) and PET/CT (C and D) images of the tarsus of a 13-year-old Quarter horse mare with 6 months duration of 3/5 left hind limb lameness. CT images show mild to moderate peri-articular remodeling at the dorsal, medial and plantar aspects of the tarsometatarsal joint. PET shows moderate activity only at the plantar aspect of the tarsometatarsal joint.

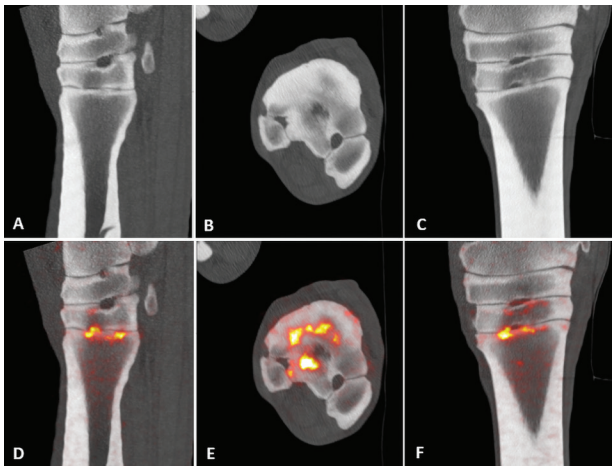

Figure 3—From left to right, sagittal, transverse and dorsal plane CT (A, B and C) and PET/CT (D, E and F) images of the left tarsus of a 9-year-old Quarter Horse mare with 3/5 bilateral hind limb lameness. No abnormal findings were recorded on CT; however, PET scan showed mild to moderate uptake preferentially located at the plantar aspect of the tarsometatarsal joint.

cystic lesion at the distal portion of the central tarsal bone with moderate uptake (SUVmax = 35.1). All the tarsi with the main lesion localized to the TMTJ presented degenerative changes on CT and mild to

moderate uptake on PET (SUVmax = 16.6; Figure 3). Two out of 4 tarsi with the main lesion localized to the PSL presented mild uptake (mean SUVmax = 17) at the plantar surface of the third metatarsal bone with minimal changes detected on CT **(Figure 4)**.

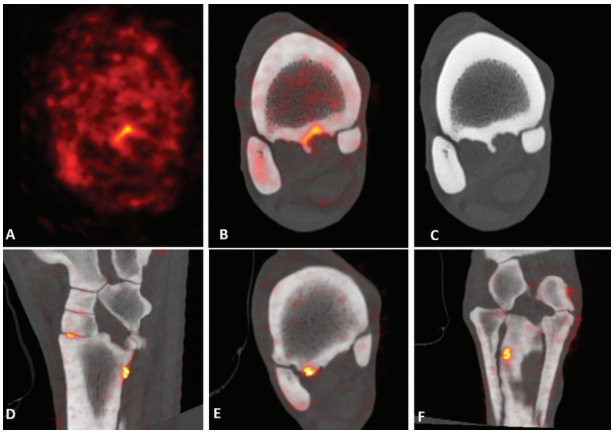

Figure 4—Two cases are presented in this figure. PET (A), PET/CT (B) and CT (C) transverse images at the level of the proximal metatarsus of a 15-year-old Warmblood gelding with chronic history of bilateral hind limb lameness. Mild PET uptake is present at the plantar cortex of the third metatarsal bone. CT showed a markedly irregular plantar margin with multiple large enthesophytes. Sagittal (D), transverse (E) and dorsal (F) multiplanar reconstruction PET/CT images of the left tarsus of a 14-year-old Warmblood mare used for show jumping that presented with 2 months duration of 3/5 right hind limb lameness. The lateral aspect of the plantar cortex of the third metatarsal bone is mildly irregular on the CT images. PET showed moderate focal uptake at this site.

The remaining 2 cases had a markedly irregular plantar surface of the third metatarsal bone with mild to moderate uptake (mean SUVmax = 13; Figure 4). The 2 tarsi with the main lesion localized to the MTB presented enostosis like lesions at the dorsal aspect of the third metatarsal bone with mild uptake (SUVmax = 14.5; **Figure 5**).

CT lesion types and SUV max

The talus background uptake for calculation of the SUVratio was 4.2 (SD = 1.3). The SUVmax and SUVratio values for CT lesions classified as enthesophytosis (mean SUVmax = 9.45, SD = 9.15; mean SUVratio = 2.62, SD = 2.1), sclerosis (mean SUVmax = 4.5, SD = 5.8; mean SUVratio = 2.6, SD = 0.9), joint fusion (mean SUVmax = 6.6, SD = 7; mean SUVratio = 2.8, SD = 2.4), bone resorption (mean SUV = 20.29, SD 13.1; mean SUVratio = 5.4, SD=2.7), and osteophytes (mean SUVmax = 11.9, SD = 4.85; mean SUVratio = 2.61, SD=0.8) are reported. The SUVmax values for CT lesions classified as bone resorption were significantly higher when compared to the remaining lesion types. No significant difference in SUVmax was found between the remaining CT lesion types ($P < .01$). Fragmentation and cyst like lesions were not included in the analysis due to the low number of lesions.

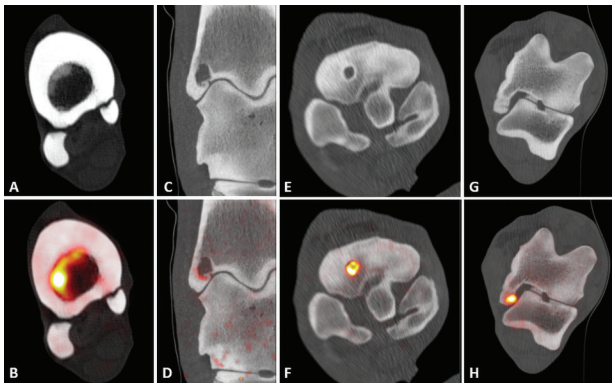

Figure 5—CT (A, C, E, G) and PET/CT (B, D, F, H) of 4 cases with lesions not associated with lameness. Transverse section images of the right proximal metatarsal region of a 13-year-old Thoroughbred gelding presenting with left hind limb lameness (A and B). There is a moderate PET uptake matching with increased mineral density of the trabecular bone consistent with enostosis. Dorsal plane images of an 8-year-old Andalusian horse without evidence of hind limb lameness (C and D). The patient was referred for potential surgical debridement or stabilization of the large cystic lesion at the lateral malleolus of the tibia with mild distal uptake on PET scan. Transverse images of the right third tarsal bone of a 12-year-old Warmblood gelding used for show-jumping presenting with a 3/5 left hind limb lameness (E and F). A cystic lesion with moderate uptake is present at the dorsal aspect of the third tarsal bone. Transverse images of the left talus of a 5-year-old Warmblood gelding used for dressage (G and H). There is partial fragmentation of the proximal tubercle of the talus with moderate uptake on PET scan. A similar lesion is present in the contralateral limb. This patient was presented with left hind limb lameness that was abolished after perineural anesthesia of the deep branch of the lateral plantar nerve. Further lameness work-up revealed pain arising from the metatarso-phalangeal region.

Association between PET and CT findings with signalment

When assessing potential associations between CT and PET scores with age, only the PET medial score was significantly and negatively correlated with age (R = 0.35; $P < .05$).

The prevalence of abnormal findings per region for Quarter Horses and Sport Horses are presented **(Figure 6)**. The Quarter Horses tend to have more common lesion of the DIT and TMTJ than the other breeds. The TTJ lesions appeared to be more common in Warmbloods and others, while the prevalence of suspensory enthesopathy appeared even. Only 2 of the 4 tarsi from Thoroughbreds had a main lesion on PET scan that was localized to the MTB.

When comparing the PET and CT scores of the distal tarsal joints of the tarsus, Quarter Horses had significantly higher PET score ($P = .03$) at the dorsal region when compared to Sport Horses. No significant differences between Quarter Horses and Sport Horses were detected for the CT score at the dorsal region. Both, PET and CT scores for the plantar region were significantly higher in Quarter Horses ($P < .05$). For the medial region, CT scores were also

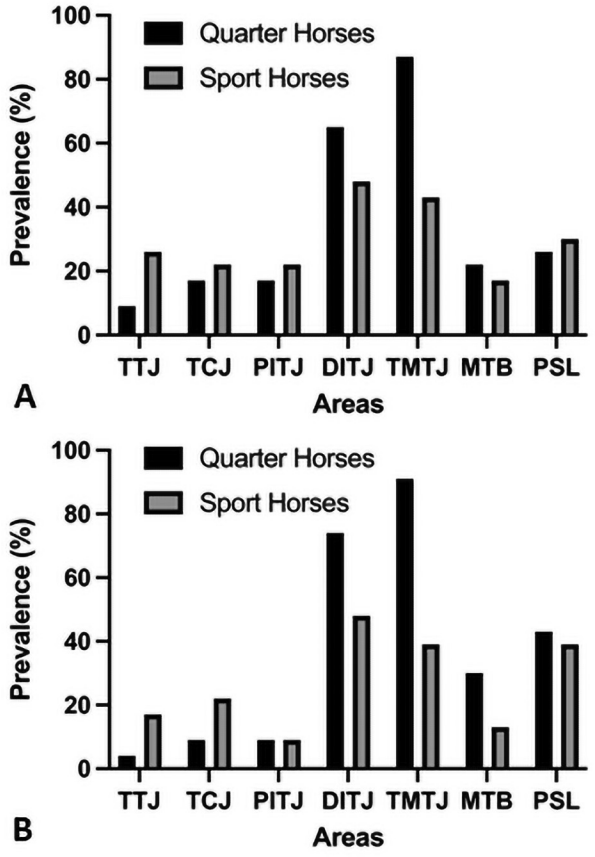

Figure 6—Prevalence of abnormal PET (A) and CT (B) findings per region for Quarter Horses and Sport Horses. The region is represented on the x-axis as follows: tibiotarsal joint (TTJ), talocalcaneal joint (TCJ), proximal intertarsal joint (PITJ), distal intertarsal joint (DITJ), tarsometatarsal joint (TMTJ), metatarsal bones (MTB; second, third and fourth metatarsal bones excluding their proximal articular portion and the enthesis of the suspensory ligament) and proximal suspensory ligament (PSL).

significantly higher in Quarter Horses ($P < .05$) and no difference between breeds was identified for the PET scores ($P = .12$). No differences between breed were detected for the CT ($P = .22$) or PET ($P = .13$) scores of the lateral region.

Association between PET and CT findings with lameness

Bilateral hind limb lameness was recorded in 8 horses. In 6/8 horses with bilateral hind limb lameness the main lesion was localized to the distal tarsal joints, and in the remaining 2/8 the main lesion was present in the proximal suspensory region. The median AAEP grade was 1 (range, 1 to 4; mean 1.6, SD 1.05). Data from objective lameness evaluation (Lameness Locator) was available in 17/25 horses. The recorded mean Max-D was 10.52 (SD 9.22) and the mean Min-D was 8.29 (SD 7.14).

The highest Spearman correlation coefficient was found between SUVratio of the main lesion and Max-D (R = 0.71, $P < .05$), followed by SUVmax of the main lesion and Max-D (R = 0.59, $P < .05$). The AAEP lameness grade was significantly correlated with the SUVmax value of the main lesion (R = 0.45, $P = .02$). There was no significant correlation between Min-D and any of the imaging related variables.

For the distal tarsal joints of the tarsus, moderate to fair Spearman correlation was found between CT and PET at the plantar region and Max-D (CT plantar grade - Max-D [R = 0.6; $P < .05$], PET plantar grade - Max-D [R = 0.47; $P = .04$]). The CT medial grade was significantly and fairly correlated with Max-D (R = 0.55; $P = .01$). No significant correlation was found between PET medial grade and Max-D. CT plantar grade was significantly fairly correlated with Min-D (R = 0.53; $P = .03$). No other correlations were detected between Min-D and PET or CT grades for the remaining regions. PET and CT grades for the dorsal and lateral regions were not correlated with any of the 3 clinical variables. AAEP lameness grade was not correlated with PET or CT grades for any of the 4 regions.

For the proximal suspensory region, abnormal PET and CT findings in nonlame limbs included fragmented tubercle of the talus (n = 1), cyst like lesion of the third tarsal bone (1), subchondral bone cyst in the distal tibia (1) and enostosis of the third metatarsal bone (2; Figure 5).

Discussion

The current study showed that ^{18}F-NaF PET was able to detect active bone remodeling associated with enthesopathy of the origin of the PSL at the proximal metatarsal region. PET also allowed to precisely identify regions of IRU at specific regions of the distal tarsal joints, talocalcaneal and tarsocrural joints. The distribution of uptake in the low motion tarsal joints significantly varied between breeds, with PET and CT changes at the plantar aspect being more prevalent in Quarter Horses and showing high correlation with objective lameness measurements.

The reported inter-observer agreement was slightly higher for PET when compared to CT but considered substantial for both modalities (PET κ = 0.66 versus CT κ = 0.6). Differences are likely related to the high lesion to background signal observed with PET scan with most of the lesions reaching an SUVratio > 2.5. We reported a significant positive correlation between PET and CT (R = 0.49) with resorptive lesions detected on CT being associated with the highest SUVmax values. However, discrepancies between the 2 modalities have also been described in the current manuscript. For the small tarsal joints, the lowest agreement was found at the level of the dorsal and medial aspect of the distal tarsal joints (weighted Kappa of 0.46 and 0.37, respectively). Several Quarter Horses had moderate dorsal and medial changes on CT with minimal to absent changes on PET scan (Figure 2). Moreover, the most common CT abnormalities was irregularity at the lateral origin of the suspensory ligament, but this only ranked as 18th for PET abnormalities. Enthesophytes located at the origin of the suspensory ligament with

^{18}F-NaF uptake are indicative of active bone remodeling. The low number of cases (4 tarsi) in which the main lesion was the PSL prevented further statistical analysis to determine possible correlation of uptake at this site with the lameness related variables. However, considering the reported moderate correlation between PET uptake (SUVmax and SUVratio) and the objective lameness assessment (Max-D) we believe that ^{18}NaF PET uptake could be used as moderately reliable marker of active painful lesions in the proximal suspensory region.

In 3 Warmbloods, moderate uptake was present at the tibia showing IRU at the joint margin with the talus. Previous reports identified similar subchondral cystic lesions using scintigraphy and CT.[20,21] Scintigraphy showed diffuse IRU distally and medially in the tibia and the authors identified the medial malleolus of the tibia as the affected portion.[20] We suspect that a similar pathology might be the origin of the uptake seen on the current cases, but the lack of resolution and the scintigraphy uniplanar images prevented proper identification of the affected region. On the above-mentioned reports CT showed precisely that the IRU was located at the medial cochlea of the tibia and that irregular periosteal new bone at the cranial or caudal tibial cortex was a common feature on these cases. Similar features were present in the included cases with this pathology (Figure 1). The initial cause of the reported changes in unclear. However, considering the acute onset of clinical signs, traumatic contusion with secondary osteonecrosis of the subchondral bone plate remains the most likely explanation. Practitioners should be aware of the described lesion type when evaluating Sport Horses with diffuse scintigraphy uptake at the distal tibia.

The current study revealed significant differences in distribution of the lesions among different breeds with PET and CT scores for the plantar region being higher in Quarter Horses when compared to Sport Horses. Several of the included Quarter Horses were used for a variety of Western performance disciplines with different athletic demands. Most of the Sport Horses were warmbloods used for show jumping or dressage. Differences in tarsal loading associated with the modality, surface and/or conformation could explain the reported differences. PET and CT grades at the plantar region showed respectively fair to moderate correlation with objective lameness scores. PET uptake at the plantar aspect of the tertiometatarsal joint was the most commonly reported PET abnormality. A previous study using cadaveric limbs of lame and nonlame horses reported greater subchondral bone thickness at the distal aspect of central tarsal bones medially when compared to laterally.[22] Another report using magnetic resonance imaging reported moderate to severe changes in signal intensity at the dorsal and aspect of the third and central tarsal bone in 3 lame horses.[23] To the authors knowledge this is the first report describing a positive fair to moderate correlation between plantar CT and PET changes with lameness severity. Whether the plantar changes are synchronous with the medial and dorsal lesions or secondary to gait alterations caused by pain remains unclear, but the reported findings suggest that early osteoarthritis affecting the dorsal and medial aspect of the distal tarsal joints resolve overtime, but plantar active bone remodeling is likely the cause of chronic pain. When assessing potential associations between CT and PET scores with age, only the PET medial score was weakly negatively correlated with age (R = 0.35; $P < .05$). The relatively uniform population of horses (middle age) is the most likely explanation for the poor correlation between age with CT and PET grades of the distal tarsal joints. Longitudinal studies with advanced cross-sectional imaging are required to further elucidate the timing of tarsal degenerative joint disease affecting the equine tarsus.

Multiple studies have tried to correlate tarsal imaging findings with lameness.[24,25] On a recent report using high field MRI to assess the tarsal region in Quarter Horses only bone marrow lesions of the third tarsal bone were positively and weakly correlated with the degree of lameness (R = 0.22).[24] In the current study, the highest correlation (R = 0.71) was found between SUVratio of the main lesion and Max-D. Using the similar subjective lameness scale (AAEP scale)[15] than in MRI study,[24] the SUVmax was also significantly but fairly correlated with lameness severity (R = 0.45). As previously discussed, plantar changes of the distal tarsal joints showed the highest (fair to moderate) correlation with objective lameness scores when compared to the other regions. In humans, ^{18}F-NaF PET uptake consistently identified painful lesions at the plantar aspect of the tarsus (os trigonum) that were frequently undetected on MRI.[26 2728]Unfortunately, no comparison with MRI nor follow up PET studies were performed in the current study. Despite the described fair to moderate correlation between PET uptake and lameness, we also report specific lesion types such as fragmentation, cystic lesions and enostosis presenting moderate PET uptake that were not associated with lameness (Figure 5). Clinicians and radiologists should consider location and lesion types when assessing the clinical relevance of ^{18}F-NaF uptake.

The main limitations of the current study include the relatively low number of cases and the retrospective nature of it. The majority of the horses included were Quarter Horses and Warmbloods making it difficult to extrapolate our findings to other breeds. Moreover, in several cases an overlap between CT lesion types was found. Magnetic resonance imaging and histology was not available in the big majority of the cases. Additionally, a standard protocol to perform diagnostic analgesia of the tarsal region was not performed and cases from multiple clinicians with different blocking patterns were included. Considering the well described lack of specificity of perineural and intra-articular diagnostic analgesia[5,24,27] of the tarsal and proximal metatarsal region this limitation is considered less relevant. Subjective lameness scores (AAEP scale) consistently had lower correlation values with CT and PET scores than objective data. This is likely caused by the retrospective nature of the study with multiple clinicians performing the lameness evaluations in the included cases.

Moreover, a control group of nonlame horses have not been used for comparison. Finally, follow-up PET scans were not performed in the included cases.

In conclusion, ^{18}F-NaF PET uptake is not equivalent to pain and thus lameness. The location of the uptake and CT changes are important factors that should be taken into consideration when evaluating cases with lameness localized to the tarsal and proximal metatarsal region. ^{18}F-NaF PET uptake located at the medial cochlea of the tibia in Warmblood horses and the plantar aspect of the distal tarsal joints in Quarter Horses had moderate correlation with lameness.

Acknowledgments

No specific funding was obtained for this study. The clinical equine PET program at UC Davis is supported by the Center for Equine Health.

The authors declare that there were no conflicts of interest.

The first author would like to express gratitude towards Concepcion Romero Jimenez for her unconditional support and family leadership.

References

1. Denoix J-M. The hock and crus. In: *The International Society Equine Locomotor Pathology.* Peninsula; 2015.
2. Butler J, Colles CM. Dyson S, Kold S, Poulos P. The tarsus. In: *Clinical Radiology of the Horse.* 3rd ed. Wiley-Blackwell; 2008:321–361.
3. Baxter GM. The tarsus and tibia. In: Baxter GM, ed. *Adams and Stashak's Lameness in Horses.* 6th ed. Wiley-Blackwell; 2011:725–782.
4. Contino EK, King MR, Valdés-Martínez A, McIlwraith CW. In vivo diffusion characteristics following perineural injection of the deep branch of the lateral plantar nerve with mepivacaine or iohexol in horses. *Equine Vet J*. 2015;47(2):230–234. doi:10.1111/evj.12261
5. Claunch KM, Eggleston RB, Baxter GM. Effects of approach and injection volume on diffusion of mepivacaine hydrochloride during local analgesia of the deep branch of the lateral plantar nerve in horses. *J Am Vet Med Assoc*. 2014;245(10):1153–1159. doi:10.2460/javma.245.10.1153
6. Murray RC, Dyson SJ, Weekes JS, Short C, Branch MV. Scintigraphic evaluation of the distal tarsal region in horses with distal tarsal pain. *Vet Radiol Ultrasound*. 2005;46(2):171–178. doi:10.1111/j.1740–8261.2005.00032.x
7. Daniel AJ, Judy CE, Rick MC, Saveraid TC, Herthel DJ. Comparison of radiography, nuclear scintigraphy, and magnetic resonance imaging for detection of specific conditions of the distal tarsal bones of horses: 20 cases (2006–2010). *J Am Vet Med Assoc*. 2012;240(9):1109–1114. doi:10.2460/javma.240.9.1109
8. Labens R, Schramme MC, Robertson ID, Thrall DE, Redding WR. Clinical, magnetic resonance, and sonographic imaging findings in horses with proximal plantar metatarsal pain. *Vet Radiol Ultrasound*. 2010;51(1):11–18. doi:10.1111/j.1740–8261.2009.01614.x
9. Spriet M, Espinosa P, Kyme A, et al. Positron emission tomography: a promising modality for imaging the equine distal limb. In: *Proceedings of the American Association of Equine Practitioners*. American Association of Equine Practitioners Annual Convention; 2016.
10. Spriet M, Espinosa P, Kyme AZ, et al. ^{18} F-sodium fluoride positron emission tomography of the equine distal limb: exploratory study in three horses. *Equine Vet J*. 2018;50(1):125–132. doi:10.1111/evj.12719
11. Spriet M, Espinosa P, Kyme AZ, et al. Positron emission tomography of the equine distal limb: exploratory study. *Vet Radiol Ultrasound*. 2016;57(6):630–638. doi:10.1111/vru.12430
12. Czernin J, Satyamurthy N, Schiepers C. Molecular mechanisms of bone 18F-NaF deposition. *J Nucl Med*. 2010;51(12):1826–1829. doi:10.2967/jnumed.110.077933
13. Spriet M, Arndt S, Pige C, et al. Comparison of skeletal scintigraphy and standing 18F-NaF positron emission tomography for imaging of the fetlock in 33 Thoroughbred racehorses. *Vet Radiol Ultrasound*. 2022;64(1):123–130.
14. Spriet M, Espinosa-Mur P, Cissell DD, et al. ^{18}F-sodium fluoride positron emission tomography of the racing Thoroughbred fetlock: validation and comparison with other imaging modalities in nine horses. *Equine Vet J*. 2019;51(3):375–383. doi:10.1111/evj.13019
15. AAEP Horse Show Committee. *Guide to Veterinary Services for Horses Shows.* 7th ed. American Association of Equine Practitioners; 1999.
16. Norvall A, Spriet M, Espinosa P, et al. Chondrosesamoidean ligament enthesopathy: prevalence and findings in a population of lame horses imaged with positron emission tomography. *Equine Vet J*. 2021;53(3):451–459. doi:10.1111/evj.13299
17. Sannajust K, Spriet M, Anishchenko S, Beylin D. Standardized uptake values and attenuation correction in ^{18} F-sodium fluoride PET of the equine foot and fetlock. *Vet Radiol Ultrasound*. 2022;63(6):771–778. doi:10.1111/vru.13127
18. McHugh ML. Interrater reliability: the kappa statistic. *Biochem Med (Zagreb)*. 2012;22(3):276–282.
19. Chan YH. Biostatistics 104: correlational analysis. *Singapore Med J*. 2003;44(12):614–619.
20. García-López JM, Kirker-Head CA. Occult subchondral osseous cyst-like lesions of the equine tarsocrural joint. *Vet Surg*. 2004;33(5):557–564. doi:10.1111/j.1532–950x.2004.04078.x
21. Raes E, Bergman HJ, Van Ryssen B, Vanderperren K, Stock E, Saunders JH. Computed tomographic features of lesions detected in horses with tarsal lameness. *Equine Vet J*. 2014;46(2):189–193. doi:10.1111/evj.12097
22. Branch MV, Murray RC, Dyson SJ, Goodship AE. Alteration of distal tarsal subchondral bone thickness pattern in horses with tarsal pain. *Equine Vet J*. 2007;39(2):101–105. doi:10.2746/042516407X166756.
23. Biggi M, Zani DD, De Zani D, Di Giancamillo M. Magnetic resonance imaging findings of bone marrow lesions in the equine distal tarsus. *Equine Vet Educ*. 2012;24(5):236–241. doi:10.1111/j.2042–3292.2011.00288.x
24. Barrett MF, Selberg KT, Johnson SA, et al. High field magnetic resonance imaging contributes to diagnosis of equine distal tarsus and proximal metatarsus lesions: 103 horses. *Vet Radiol Ultrasound*. 2018;59(5):587–596.
25. Byam-Cook KL, Singer ER. Is there a relationship between clinical presentation, diagnostic and radiographic findings and outcome in horses with osteoarthritis of the small tarsal joints? *Equine Vet J*. 2009;41(2):118–123. doi:10.2746/042516408X345107.
26. Fischer DR, Maquieira GJ, Espinosa N, et al. Therapeutic impact of [(18)F]fluoride positron-emission tomography/computed tomography on patients with unclear foot pain. *Skeletal Radiol*. 2010;39(10):987–997. doi:10.1007/s00256-010-0875-7
27. Hughes TK, Eliashar E, Smith RK. In vitro evaluation of a single injection technique for diagnostic analgesia of the proximal suspensory ligament of the equine pelvic limb. *Vet Surg*. 2007;36(8):760–764. doi:10.1111/j.1532–950X.2007.00333.x

Supplementary Materials

Supplementary materials are posted online at the journal website: avmajournals.avma.org